Mimicking anti-correlations with classical interference

2013 Phys. Scr. 2013 014030

(http://iopscience.iop.org/1402-4896/2013/T153/014030)

IOP PUBLISHING PHYSICA SCRIPTA

Phys. Scr. **T153** (2013) 014030 (4pp) doi:10.1088/0031-8949/2013/T153/014030

Mimicking anti-correlations with classical interference

S Godoy, B Seifert and S Wallentowitz

Facultad de Física, Pontificia Universidad Católica de Chile, Casilla 306, Santiago 22, Chile

E-mail: sugodoy@uc.cl

Received 17 September 2012
Accepted for publication 27 September 2012
Published 28 March 2013
Online at stacks.iop.org/PhysScr/T153/014030

Abstract
It is shown how classical laser light impinging on a beam splitter with internal reflections may mimic anti-correlations of the detected outputs, similar to those observed for anti-bunched light. The experimentally observed anti-correlation may be interpreted as a classical Hong–Ou–Mandel dip.

PACS numbers: 42.50.Ar, 42.25.Hz

(Some figures may appear in color only in the online journal)

1. Introduction

Splitting a stationary optical beam into two parts and observing anti-correlation between the detected parts is commonly believed to be a sufficient condition to attribute anti-bunching to the incident light beam. This is based on the classical treatment of the correlation function together with the application of the Cauchy–Schwartz inequality, leading to the inequality [1]

$$G(\tau) \leqslant G(0). \quad (1)$$

The violation of this inequality has been experimentally shown for the first time in [2].

Here, we argue that the violation of (1) is only a necessary but not sufficient condition for anti-bunching in the incident light. We show both theoretically and experimentally that a classical laser source can violate (1) when the beam splitter shows interference effects by internal reflections. Then the setup becomes equivalent to a classical version of the Hong–Ou–Mandel interferometer [4] with two filtered coherent input fields. The observed violation of (1) may then be interpreted as a kind of classical Hong–Ou–Mandel dip.

2. Theory

Assume a general four-port interferometer where a light beam with central frequency $\bar{\omega}$ and spectral width $\Delta\omega$ and vacuum enter input ports 1 and 2, respectively, see figure 1. Photo detection of the input field 1, being described by the bosonic mode operators $\hat{a}_\lambda$ with discrete frequencies $\omega_\lambda = \lambda \cdot \delta\omega$ ($\lambda = 0, 1, 2, \ldots$), would reveal the statistics of the photon number,

$$\hat{N}_{\mathrm{in},1}(t) = \mathcal{N} \sum_{\lambda,\lambda'} \hat{a}^\dagger_{\lambda'} \hat{a}_\lambda \mathrm{e}^{\mathrm{i}(\omega_\lambda - \omega_{\lambda'})t}, \quad (2)$$

which is accumulated during the response time τ_{det} of the detector. It is supposed that $\tau_{\mathrm{det}} \ll \tau_{\mathrm{coh}}$, where the coherence time of the light is $\tau_{\mathrm{coh}} = 2\pi/\Delta\omega$ so that $\mathcal{N} = c\epsilon_0 \tau_{\mathrm{det}} \int \mathrm{d}A |E(x, y)|^2/\hbar\bar{\omega}$ with the transverse beam profile, $E(x, y)$, being integrated over the area of the photo detector (PD).

The two output fields 1′ and 2′ are incident on PD1 and PD2 with the output photon numbers accumulated during the response time τ_{det} being ($i = 1, 2$)

$$\hat{N}_{\mathrm{out},i}(t) = \mathcal{N} \sum_{\lambda,\lambda'} f_i(\omega_\lambda, \omega_{\lambda'}) \hat{a}^\dagger_{\lambda'} \hat{a}_\lambda \mathrm{e}^{\mathrm{i}(\omega_\lambda - \omega_{\lambda'})t} + \text{vacuum terms}. \quad (3)$$

The interferometric structure is encoded by the functions $f_i(\omega, \omega')$, which are restricted by the relations $f_i(\omega, \omega') = f_i^*(\omega', \omega)$, imposed by the Hermiticity of the photon numbers (3). Note that the 'vacuum terms' contain mode operators of the vacuum field at input port 2.

Recording the traces of the outputs of PD1 and PD2, the normally ordered cross correlation of photon numbers,

$$G_{\mathrm{out}}(t_1, t_2) = \langle : \hat{N}_{\mathrm{out},1}(t_1) \hat{N}_{\mathrm{out},2}(t_2) : \rangle, \quad (4)$$

is obtained by statistically averaging the product of time-delayed traces. For stationary light at input port 1, the

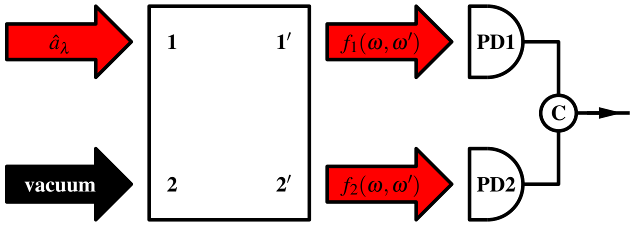

Figure 1. A four-port interferometer with a classical light field at input 1 and vacuum at input 2.

correlation (4) only depends on the difference time $\tau = t_1 - t_2$ and is obtained from (3) and (4) as [1]

$$G_{\rm out}(\tau) = \mathcal{N}^2 \sum_{\mu=-\infty}^{\infty} \sum_{\lambda,\lambda'=\max(0,\mu)}^{\infty} {\rm e}^{{\rm i}\omega_\mu \tau} f_1(\omega_\lambda, \omega_{\lambda-\mu}) \times f_2(\omega_{\lambda'-\mu}, \omega_{\lambda'}) \left\langle : \hat{a}^\dagger_{\lambda-\mu} \hat{a}_\lambda \hat{a}^\dagger_{\lambda'} \hat{a}_{\lambda'-\mu} : \right\rangle . \quad (5)$$

The functions f_i may contain parts g_i that only depend on the difference frequency,

$$f_i(\omega, \omega - \nu) = g_i(\nu) + \varepsilon_i(\nu, \omega), \quad (6)$$

with ε_i being terms that additionally depend on ω. Using (6) the correlation (5) becomes an expansion in powers of ε_i,

$$G_{\rm out}(\tau) = G^{(0)}_{\rm out}(\tau) + G^{(1)}_{\rm out}(\tau) + G^{(2)}_{\rm out}(\tau), \quad (7)$$

where the zero-order term is obtained as

$$G^{(0)}_{\rm out}(\tau) = \sum_{\mu=-\infty}^{\infty} g_1(\omega_\mu) g_2(-\omega_\mu) \frac{1}{T} \int_{-T}^{T} {\rm d}\tau' {\rm e}^{{\rm i}\omega_\mu(\tau-\tau')} G_{{\rm in},1}(\tau'), \quad (8)$$

with $T = 2\pi/\delta\omega$. Here $G_{{\rm in},1}(\tau) = \langle : \hat{N}_{{\rm in},1}(t+\tau) \hat{N}_{{\rm in},1}(t) : \rangle$ is the correlation of the light source. It is assumed to be perfect laser light, i.e. $G_{{\rm in},1}(\tau) = {\rm const}$, leading to

$$G^{(0)}_{\rm out}(\tau) = 4(\mathcal{N}\bar{N})^2 g_1(0) g_2(0), \quad (9)$$

with $\bar{N}$ being the mean photon number of the light source accumulated during $\tau_{\rm det}$.

For the evaluation of the first- and second-order terms in the expansion (7), we first calculate the normally ordered expectation value of (5) using the density operator of a quasi-monochromatic stationary laser field,

$$\hat{\varrho} = \sum_{\{N_\lambda\}} P(\{N_\lambda\}) |\{N_\lambda\}\rangle\langle\{N_\lambda\}|, \quad (10)$$

where $|\{N_\lambda\}\rangle$ are Fock states and the probability to observe the set of photon numbers $\{N_\lambda\}$ reads

$$P(\{N_\lambda\}) = \prod_\lambda \frac{(\bar{N}_\lambda)^{N_\lambda} {\rm e}^{-\bar{N}_\lambda}}{N_\lambda !}, \quad (11)$$

with $\bar{N}_\lambda$ being the mean photon number at frequency ω_λ. Using (10) and (11), the expectation value becomes

$$\left\langle : \hat{a}^\dagger_{\lambda-\mu} \hat{a}_\lambda \hat{a}^\dagger_{\lambda'} \hat{a}_{\lambda'-\mu} : \right\rangle = \left[\delta_{\mu,0} + (1-\delta_{\mu,0})\delta_{\lambda,\lambda'}\right] \bar{N}_\lambda \bar{N}_{\lambda'-\mu}. \quad (12)$$

Inserting (12) into (5) and performing the continuum limit $\delta\omega \to 0$ by defining the spectral photon-number density $\bar{n}(\omega_\lambda) = \lim_{\delta\omega\to 0} \bar{N}_\lambda/\delta\omega$ with mean $\bar{\omega}$ and width $\Delta\omega$ ($\Delta\omega \ll \bar{\omega}$), the first- and second-order contributions are obtained as

$$\begin{aligned} G^{(1)}_{\rm out}(\tau) = \mathcal{N}^2 \int_{-\infty}^{\infty} {\rm d}\omega \int_{-\infty}^{\infty} {\rm d}\omega' \bar{n}(\omega)\bar{n}(\omega') & \\ \times \big\{ g_1(0)\varepsilon_2(0,\omega') + g_2(0)\varepsilon_1(0,\omega) & \\ + {\rm e}^{{\rm i}(\omega-\omega')\tau} \big[g_1(\omega-\omega')\varepsilon_2(\omega'-\omega,\omega') & \\ + g_2(\omega'-\omega)\varepsilon_1(\omega-\omega',\omega) \big] \big\} , & \quad (13) \end{aligned}$$

$$\begin{aligned} G^{(2)}_{\rm out}(\tau) = \mathcal{N}^2 \int_{-\infty}^{\infty} {\rm d}\omega \int_{-\infty}^{\infty} {\rm d}\omega' \bar{n}(\omega)\bar{n}(\omega') [\varepsilon_1(0,\omega)\varepsilon_2(0,\omega') & \\ + {\rm e}^{{\rm i}(\omega-\omega')\tau} \varepsilon_1(\omega-\omega',\omega)\varepsilon_2(\omega'-\omega,\omega')]. & \quad (14) \end{aligned}$$

The function ε_i can be represented as the sum over interferometric phase factors,

$$\varepsilon_i(\nu, \omega) = \sum_k \varepsilon_{i,k} {\rm e}^{{\rm i}\nu\tau_{i,k}} {\rm e}^{{\rm i}\omega t_{i,k}}, \quad (15)$$

where $\varepsilon_{i,j}$ are amplitudes and $\tau_{i,k}$ and $t_{i,k}$ are time lags of optical paths within the interferometer, which are assumed to be $\tau_{i,k}, t_{i,k} \ll \tau_{\rm coh}$. In this way, the contributions (13) and (14) can be rewritten as

$$\begin{aligned} G^{(1)}_{\rm out}(\tau) = (\mathcal{N}\bar{N})^2 \sum_k \Big\{ & [\varepsilon_{2,k} {\rm e}^{{\rm i}\bar{\omega}t_{2,k}} \underline{g}_1(0) + \varepsilon_{1,k} {\rm e}^{{\rm i}\bar{\omega}t_{1,k}} \underline{g}_2(0)] \\ & + \int {\rm d}t |P_0(t)|^2 [\varepsilon_{2,k} {\rm e}^{{\rm i}\bar{\omega}t_{2,k}} \underline{g}_1(t+\tau-\tau_{2,k}) \\ & + \varepsilon_{1,k} {\rm e}^{{\rm i}\bar{\omega}t_{1,k}} \underline{g}_2(t-\tau-\tau_{1,k})] \Big\}, \end{aligned} \quad (16)$$

$$G^{(2)}_{\rm out}(\tau) = (\mathcal{N}\bar{N})^2 \sum_{k,l} \varepsilon_{1,k}\varepsilon_{2,l} {\rm e}^{{\rm i}\bar{\omega}(t_{1,k}+t_{2,l})} \left[1 + |P_0(\tau)|^2\right], \quad (17)$$

where we defined the Fourier transform

$$\underline{g}_i(t) = \frac{1}{2\pi} \int {\rm d}\omega {\rm e}^{-{\rm i}\omega t} g_i(\omega), \quad (18)$$

and the Fourier transform of the normalized and centred photon-number spectrum,

$$P_0(t) = \frac{1}{\bar{N}} \int {\rm d}\omega {\rm e}^{-{\rm i}\omega t} \bar{n}(\omega + \bar{\omega}). \quad (19)$$

Its temporal width around its peak value at $t = 0$ is given by the coherence time $\tau_{\rm coh}$ of the light source.

From (16) and (17), it can be seen that interference effects occur that generate a time dependence of the intensity correlation function. This time dependence appears in the form of the Fourier transformed spectral intensity $P_0(t)$ that has a width given by the coherence time of the incident light. As a consequence, the time dependence of the intensity correlation vanishes for a perfectly monochromatic light source.

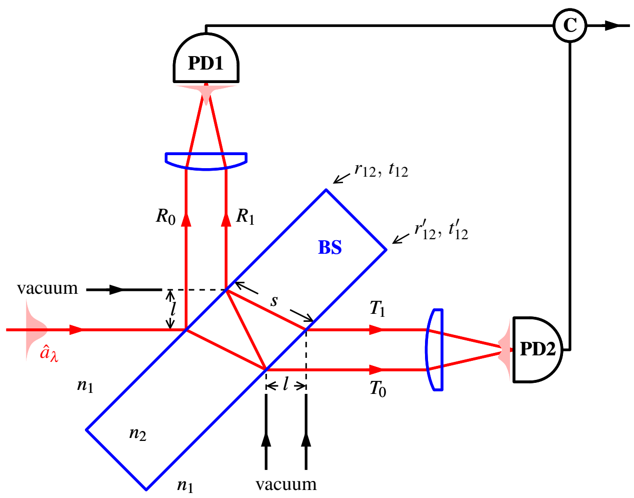

Figure 2. Beam splitter (BS) with principal optical paths R_0 and T_0 and internally reflected additional optical paths R_1 and T_1 in reflection and transmission, respectively.

3. Beam splitter with internal reflections

A beam splitter without anti-reflection (AR) coating has reflectivity and transmittance coefficients for the direct reflection and transmission,

$$R_0 = r_{12}, \quad T_0 = t_{12}t'_{21}, \tag{20}$$

and reflectivity and transmittance for the (first-order) internally reflected contributions (ghosting),

$$R_1 = t_{12}r'_{21}t_{21}, \quad T_1 = t_{12}r'_{21}r_{21}t'_{21}, \tag{21}$$

where r_{ij} (t_{ij}) and r'_{ij} (t'_{ij}) are the electric-field reflection (transmission) coefficients for the first and the second surface of the beam splitter, respectively, see figure 2.

For this case the functions characterizing the interferometric effects in the two output channels are[1]

$$f_1(\omega, \omega-\nu) = |T_0|^2 + |T_1|^2 \mathrm{e}^{\mathrm{i}\nu\tau_{\mathrm{bs}}} + T_0^* T_1 \mathrm{e}^{\mathrm{i}\omega\tau_{\mathrm{bs}}} + T_0 T_1^* \mathrm{e}^{-\mathrm{i}(\omega-\nu)\tau_{\mathrm{bs}}}, \tag{22}$$

$$f_2(\omega, \omega+\nu) = |R_0|^2 + |R_1|^2 \mathrm{e}^{\mathrm{i}\nu\tau_{\mathrm{bs}}} + R_0^* R_1 \mathrm{e}^{\mathrm{i}\omega\tau_{\mathrm{bs}}} + R_0 R_1^* \mathrm{e}^{-\mathrm{i}(\omega-\nu)\tau_{\mathrm{bs}}}, \tag{23}$$

where the time delay between direct and internally reflected beams is $\tau_{\mathrm{bs}} = (l-2s)/c$. The incoherent contributions are identified from (6) as the first two terms in (22) and (23), respectively, with its Fourier transforms being

$$\underline{g}_1(t) = |T_0|^2 \delta(t) + |T_1|^2 \delta(t-\tau_{\mathrm{bs}}), \tag{24}$$

$$\underline{g}_2(t) = |R_0|^2 \delta(t) + |R_1|^2 \delta(t-\tau_{\mathrm{bs}}). \tag{25}$$

The remaining terms in (22) and (23) correspond to interference effects, resulting in the amplitudes $\varepsilon_{1,1} = \varepsilon_{1,2}^* = T_0^* T_1$, $\varepsilon_{2,1} = \varepsilon_{2,2}^* = R_0^* R_1$ and non-zero time lags $t_{i,1} = -t_{i,2} = \tau_{i,2} = \tau_{\mathrm{bs}}$ $(i = 1, 2)$. Inserting these coefficients together with (24) and (25) into the three contributions (9), (16) and (17), the complete correlation is obtained as[2]

$$G_{\mathrm{out}}(\tau) = 4(\mathcal{N}\bar{N})^2 \left(|T_0|^2 + |T_1|^2\right)\left(|R_0|^2 + |R_1|^2\right) \times \left\{1 + A\left[1 + |P_0(\tau)|^2\right]\right\}, \tag{26}$$

where the relative amplitude of the interference contribution is[3]

$$A = -\kappa_{\mathrm{r}}\kappa_{\mathrm{t}}\xi^2 + \frac{\kappa_{\mathrm{r}} - \kappa_{\mathrm{t}}}{2}\xi \tag{27}$$

with the three independent parameters

$$\xi = \cos\left[\arg\left(R_0^* R_1\right) + \bar{\omega}\tau_{\mathrm{bs}}\right], \tag{28}$$

and

$$\kappa_{\mathrm{r}} = \frac{|R_0 R_1|}{|R_0|^2 + |R_1|^2}, \quad \kappa_{\mathrm{t}} = \frac{|T_0 T_1|}{|T_0|^2 + |T_1|^2}. \tag{29}$$

The interference terms in (26) ($\propto A$) establish an extrema at $\tau = 0$ with the width being proportional to the coherence time of the light source. This extrema can be a maximum ('bunching') or minimum ('anti-bunching') depending on the sign of A.[4] The maximum anti-correlation (i.e. $A < 0$) can be obtained for $\kappa_{\mathrm{t}} \gtrless \kappa_{\mathrm{r}}$ when $\xi = \pm 1$, for which $A = -\kappa_{\mathrm{r}}\kappa_{\mathrm{t}} - |\kappa_{\mathrm{r}} - \kappa_{\mathrm{t}}|/2$.

4. Experimental results

The light source was a tunable external cavity diode laser [3] using a laser diode (Sanyo DL-7140-201s) and a diffraction grating (Thorlabs GH25-18 V) with 1800 grooves/mm at a distance of approximately 6 cm. Part of the laser light (3.2 mW @ 785 nm) is incident on a low-absorption near-IR beam-splitter plate (Edmund Optics NT48-903) with multi-layer AR coating optimized for random polarization at 45° angle of incidence. As S polarization is chosen, the incidence angle for obtaining balanced outputs is approximately 7° and the AR coating is to a large extent disabled, allowing for internal reflection. The transmitted and reflected light is then focused onto two Si PIN photo diodes (Hamamatsu S3883) with transimpedance amplifiers (Hamamatsu C8366). The output voltages are recorded with two channels of a digital oscilloscope (LeCroy WJ354A) at a sampling rate of 1 GHz.[5]

Each trace of the measured data contains 100 000 data points from which the correlation is calculated. The resulting normalized correlation

$$\tilde{G}_{\mathrm{out}}(\tau) = \frac{G_{\mathrm{out}}(\tau) - G_{\mathrm{out}}(\infty)}{G_{\mathrm{out}}(\infty)} \tag{30}$$

[1] For notational simplicity we choose identical optical paths from the point of incidence of the light field to the two detectors and take the point of incidence as zero phase reference.

[2] Note that $\tau_{\mathrm{bs}} \ll \tau_{\mathrm{coh}}$ so that the approximations made for obtaining (16) and (17) are justified.

[3] Here we employed $T_0^* T_1 = -|t'_{21}|^2 R_0^* R_1$, which results from the Stokes relations of the reflecting surfaces.

[4] Note that for $\tau_{\mathrm{coh}} \to \infty$, i.e. for a perfectly monochromatic source, the correlation function becomes a constant.

[5] dc values are measured separately from ac values (1 MHz high pass filter). Systematic errors where $\pm(1.5\% + 0.5\%$ full scale) with full scale being 2 V (dc) and 100 mV (ac), respectively.

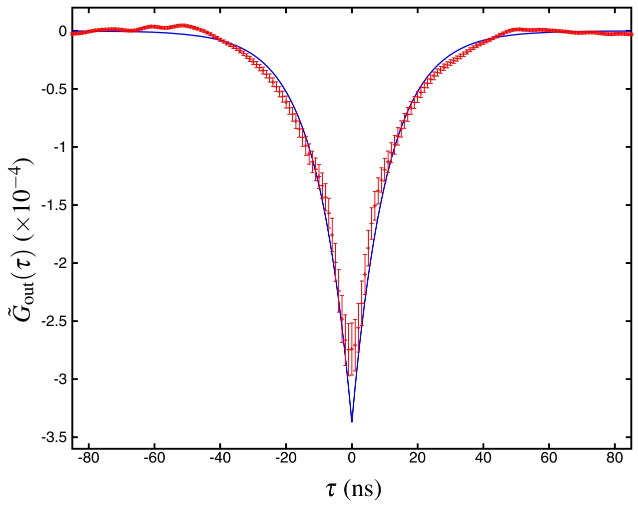

Figure 3. Normalized correlation $\tilde{G}_{\rm out}(\tau)$ determined from the measured data with error bars containing systematic and statistical errors. The blue curve shows a least-squares fit to the Fourier transform of a Lorentzian spectrum.

is shown in figure 3. It is fitted well assuming a Lorentzian spectral photon-number distribution of the light source,

$$\bar{n}(\omega) = \frac{\bar{N}}{\pi}\left[\frac{\Delta\omega}{(\omega-\bar{\omega})^2+\Delta\omega^2}\right], \tag{31}$$

from which the normalized correlation results as

$$\tilde{G}_{\rm out}(\tau) = \frac{A}{1+A}\exp\left(-2\Delta\omega\,|t|\right). \tag{32}$$

Deviations from this curve are observed for a range of 10 ns delay time around the peak, which corresponds to the bandwidth limitation of 100 MHz of the photo detectors. From the width of the fitted peak, the laser line width is determined as $\Delta\omega/2\pi \approx 7.4$ MHz, which corresponds to the coherence time $\tau_{\rm coh} \approx 135$ ns and is in perfect agreement with the laser setup used.

5. Discussion and conclusions

From the measured correlation, cf figure 3, following inequality (1) one could infer anti-bunching in the incident light beam. However, our light source is classical laser light both in experiment and in the presented theory, which perfectly matches the experimental results. Therefore, a reason must exist for which (1) may not be applicable here. It is identified by reproducing the derivation of (1):

Classically, the cross-correlation function is given by $G_{12}(\tau) = \overline{N_1(t+\tau)N_2(t)}$, where $N_i(t)$ is the time-integrated optical flux at the photo detector i ($i = 1, 2$). A classical joint probability $P(N_1, t+\tau; N_2, t)$ for the detection of N_1 and N_2 at times $t+\tau$ and t, respectively, allows for the application of the Cauchy–Schwartz inequality, which leads to

$$G_{12}(\tau) \leqslant \sqrt{G_{11}(0)G_{22}(0)}, \tag{33}$$

assuming stationary light. For obtaining (1) from (33) it must be assumed that

$$N_i(t) = k_i N(t), \tag{34}$$

i.e. the $N_i(t)$ $(i = 1, 2)$ are proportional to a common statistical process $N(t)$. Under this assumption the indices of the correlations become irrelevant, i.e. $G_{ij}(\tau) \to G(\tau)$ becomes an auto-correlation, and (1) is obtained.

Equation (34) requires a perfectly flat frequency response of the beam splitter within the spectral range of the incident light. Thus, for applying the condition (1) in order to proof anti-bunching in the incident light beam it is therefore only necessary but not sufficient to observe anti-correlations between the split output beams. Additionally, one must proof that the beam splitting is done according to condition (34).

The effects seen here are somewhat similar to the Hong–Ou–Mandel dip [4]. In fact, our system is equivalent to a perfect balanced beam splitter with two filtered coherent input fields, for which a classical Hong–Ou–Mandel dip would be expected for the case $\tau_{\rm det} \gg \tau_{\rm coh}$. However, our coherence time supersedes the detection time. Possibly, this is compensated for by the spectral difference between the two equivalent input fields, which read $\hat{a}_\pm(\omega) = \hat{a}(\omega)[(R_0 + R_1 e^{i\omega\tau_{\rm bs}}) \pm (T_0 + T_1 e^{i\omega\tau_{\rm bs}})]/\sqrt{2}$. In this sense the observed anti-correlation may be similar to a classically generated Hong–Ou–Mandel dip, such as implemented with time delay [5], dispersion [6] or anti-correlated chirped light [7, 8].

Acknowledgments

This research was supported by FONDECYT project no. 1095214. SG acknowledges support from the doctoral fellowship Ayudante Becario VRI PUC.

References

[1] Mandel L and Wolf E 1995 *Optical Coherence and Quantum Optics* (Cambridge: Cambridge University Press)
[2] Kimble H J, Dagenais M and Mandel L 1977 *Phys. Rev. Lett.* **39** 691
[3] Ye C 2004 *Tunable External Cavity Diode Lasers* (Singapore: World Scientific)
[4] Hong C K, Ou Z Y and Mandel L 1987 *Phys. Rev. Lett.* **59** 2044
[5] Legero T, Wilk T, Kuhn A and Rempe G 2003 *Appl. Phys.* B **77** 797
[6] Resch K J, Puvanathasan P, Lundeen J S, Mitchell M W and Bizheva K 2007 *Opt. Express* **15** 8797
[7] Kaltenbaek R, Lavoie J, Biggerstaff D N and Resch K J 2008 *Nature Phys.* **4** 864
[8] Kaltenbaek R, Lavoie J and Resch K J 2009 *Phys. Rev. Lett.* **102** 243601